

Analysis and Design of a Directive Antenna Array for C-Band Communication Applications

Ayman Elboushi^{1,2}, Anwer S. Abd El-Hameed^{1,*}, Sulaiman Alsuwailem², and Eman G. Ouf¹

¹Electronics Research Institute, Cairo, Egypt

²Prince Sultan Defense Studies and Research Center, Saudi Arabia

ABSTRACT: Three scenarios of high gain bow-tie based antenna array systems are introduced and investigated in this paper. The proposed designs are intended for integration as Tx/Rx antennas in C-band communication systems. Wide operating bandwidth and consistent radiation characteristics over the frequency range from 4 GHz to 5 GHz are defined for the three configurations. A two-stage Wilkinson power divider provides the feed mechanism for the proposed array. The initial structure has four radiating elements, each incorporating seven bow-tie dipoles arranged in a printed Log-Periodic Directional Array (PLPDA) configuration. The gain of the second and third designs is improved by adding resonators in front of the array elements. Furthermore, the second design features triangular-shaped resonators, while the third design employs H-shaped resonators. The designs are simulated and optimized using HFSS and CSTMWS software, and subsequently, they are fabricated using the photolithography technique. The initial design demonstrates an experimental bandwidth from 3.7 GHz to 5.1 GHz and achieves a measured gain of 13.8 dBi at 4.7 GHz. The second and third configurations operate in the frequency bands of 4.3 GHz to 5.3 GHz and 3.7 GHz to 5 GHz, respectively, exhibiting measured gains of 14.1 dBi and 15 dBi. The overall dimensions of the proposed arrays are kept within reasonable limits, with the first array being $2.51\lambda \times 2.74\lambda$, the second being $2.09\lambda \times 2.82\lambda$, and the third being $2.51\lambda \times 2.97\lambda$. The three array designs can be considered as good candidates for C-band communication applications.

1. INTRODUCTION

In recent times, there is a growing interest in creating high-gain antennas with broad bandwidth to cater to the demands of various wireless applications [1–5]. Log Periodic Dipole Array (LPDA) is a type of antenna system that is designed to provide a wide frequency range while maintaining directivity and gain. It was first developed in the 1960s and has since been used in various applications such as broadcasting, radar systems, and telecommunications [6]. The mechanism of LPDA antenna design to evaluate the spacing factor and scaling factor is discussed in [6]. The key feature of the Log Periodic Directional Array is its ability to cover a wide range of frequencies without the need for multiple antennas or frequency specific elements. It achieves this through a unique design consisting of a series of dipole elements that decrease in size as the frequency increases.

Log Periodic Directional Array (LPDA) consists of numerous dipoles of varying lengths, arranged in a specific geometric pattern [7]. This arrangement allows the antenna to exhibit a constant impedance and radiation pattern over a wide frequency range. The dipole elements are spaced in a way that the spacing becomes larger as the frequency decreases, giving the antenna its log periodic characteristics.

There are several different shapes of dipole antenna, such as straight half-wave dipole, folded dipole, inverted V dipole,

circular dipole, elliptical dipole, and bow-tie dipole [8–13]. Straight half-wave dipole is the simplest form of dipole antenna, consisting of a straight rod or wire of half the wavelength of the desired signal. Folded dipole consists of a straight rod or wire folded back on itself to form a loop. The impedance and bandwidth of a folded dipole are typically higher than that of a straight dipole. Inverted V dipole is a variation of the straight dipole where the two ends of the antenna are bent downwards in a V shape. This shape is often used where horizontal installation space is limited. Circular dipole is a complete circle, rather than straight or folded. It is often used in applications such as circularly polarized antennas. Elliptical dipole is an ellipse rather than a complete circle. This shape is often used to achieve specific radiation patterns or polarization characteristics. Bow-tie dipole consists of two triangular-shaped elements arranged in a bow-tie configuration [14]. It is used in broadband applications such as TV antennas. The shape of a dipole antenna plays an important role in determining its radiation pattern and performance. The two main factors affected by the shape of a dipole antenna are directivity and bandwidth. It is worth noting that the desired frequency or wavelength of operation and specific requirements of the application dictate the shape and dimensions of a dipole antenna. A typical LPDA antenna should be half the length of its lowest operating wavelength. This makes it unsuitable for space-constrained applications like aircraft and vehicle platforms. Miniaturization of the

* Corresponding author: Anwer S. Abd El-Hameed (anwer.sayed@ejust.edu.eg).

antenna is required to enable the LPDA antenna to be used on these platforms.

Several techniques have been introduced to miniaturize the LPDA antenna [15–18]. Wang et al. proposed a fractal tree LPDA antenna [15], and Anagnostou et al. applied Koch's fractal to an LPDA antenna [16]. In [17], Chen et al. proposed a top-loaded LPDA antenna in a T-shape. A compact dielectric loaded LPDA antenna is the work of Chang et al. [18]. A greater degree of miniaturization is achieved with these antennas than that with typical LPDA antennas. However, their gain is not as high as that of typical LPDA antennas. The gain of an LPDA antenna was improved by using additional elements [19, 20]. In [19], Hsu and Huang used parasitic elements as a director in an LPDA antenna with a Koch shape. However, the antenna gain characteristics were still inferior to those of a typical LPDA antenna. A dielectric lens LPDA antenna was presented by Haraz et al. [20]. This antenna is able to achieve a higher gain than that of a typical LPDA but is bulky and difficult to manufacture.

Metamaterials have properties not found in nature. They are extensively used in antenna technology [21, 22]. In particular, Sievenpiper et al. [23] proposed a metamaterial called artificial magnetic conductor (AMC), which has a periodic structure. AMC is often used for antenna miniaturization and gain enhancement [24–26]. In [27], a compact and low-profile log-periodic meander dipole array (LPMDA) antenna with an AMC is presented. The meandering configuration of the dipole elements reduces the size of the antenna by about 30%. The use of the AMC also improves the main beam gain within the bandwidth of operating frequency from 3.94–7.17 dBi to 7.86–10.01 dBi. A metamaterial loaded antenna array with 16 printed log periodic elements for microwave imaging for breast tumour detection was introduced in [28]. In order to attain a maximum gain of 5.5 dBi, an impedance bandwidth of 3 GHz (2–5 GHz), and a reflection coefficient of less than -10 dB, this antenna design is initially developed using a PLPA structure and subsequently a 1×6 metamaterial unit cell array. A bow-tie antenna has several advantages over a straight dipole. Bow-tie antennas typically have a wider bandwidth than straight dipole antennas [14]. This means that they can operate effectively over a wider range of frequencies. The bow-tie design allows better impedance matching to the transmitter/receiver feed line, resulting in increased efficiency and reduced signal loss. Bow-tie antennas tend to have a more directional radiation pattern, which means that they can focus signals in a specific direction. This can be useful in scenarios where a specific signal needs to be received or transmitted in a particular direction with increased gain. The directional nature of the bow-tie antenna helps to reduce interference from unwanted signals in unwanted directions. This can improve signal to noise ratio and overall performance. Bow-tie antennas can be made more compact than straight dipole antennas, making them suitable for applications where space is limited. The geometry of the bow-tie design helps to minimize signal reflections caused by multipath propagation, resulting in better signal quality. The benefits of bow-tie antennas make them popular for a wide range of applications, including broadcast, radio astronomy, and wireless communications systems.

In this article, the analysis and design of a directive antenna array for C-band communication applications is presented. Such an antenna can increase the communication link S/N ratio enabling longer wireless communication distance. Printed Log Periodic Directional Array (PLPDA) is a type of a directive antenna system that is more suitable for C-band applications due to its high gain and directivity. Moreover, the PLPDA offers size reduction due to velocity reduction of the propagation wave inside the substrate material. Three designs of PLPDA arrays are presented: Firstly, a 4-element PLPDA bow-tie based array is designed based on the bow-tie configuration to achieve a maximum gain of 13.8 dBi and an impedance bandwidth of 1.4 GHz (3.7–5.1 GHz) with a reflection coefficient of less than -10 dB. Secondly, a 4-element PLPDA bow-tie antenna with triangular loading is designed to achieve a maximum gain of 14.1 dBi and an impedance bandwidth of 1 GHz (4.3–5.3 GHz) with a reflection coefficient of less than -10 dB. Finally, a 4-element array of PLPDA bow-tie dipoles with H loading is formed, which achieves a maximum gain of 15 dBi and an impedance bandwidth of 1.3 GHz (3.7–5 GHz) with a reflection coefficient of less than -10 dB. ANSYS-HFSS software and CST MWS version 2021 are used to perform all simulations in this study. All the proposed antennas are verified experimentally. The proposed antenna design is presented in Section 2. Section 3 introduces a comparison between the measured and simulated results. Finally, the conclusion is presented in Section 4.

2. THE ANTENNA DESIGN

The primary objective of this work is the design and realization of a directive antenna array for C-band communication applications. Accordingly, LPDA is chosen as it provides a wide operating frequency range with high directivity and gain. Firstly, a 4-element PLPDA array structure based on a bow-tie antenna is designed, followed by the construction of a 4-element PLPDA array with a triangular loading resonator, and then the 4-element PLPDA array with H-loading resonators is presented. Printed Wilkinson power dividers are used to feed the proposed antenna array designs. Both the feeding system and antenna arrays are etched on the same substrate of Roger RT5870 (Lossy) with dielectric constant $\epsilon_r = 2.33$, loss tangent $\tan \delta = 0.0012$, and the height of $h = 0.7874$ mm.

2.1. Array Feeding Network

In order to attain a proper feeding mechanism for the antenna arrays, a Wilkinson power divider is adopted. The feed network illustrated in Fig. 1 consists of three equal power dividers arranged in two cascaded stages. A 100 Ohm resistor is placed between power divider arms to provide proper output port isolation. The optimized dimensions of the 1–4 power dividers are given in Table 1. The simulation results for the S -parameters of the 1 to 4 power divider are plotted in Fig. 2. The insertion loss of the power divider does not exceed 0.25 dB over the operating band (3.6 GHz to 5.4 GHz). Furthermore, the input port return loss is below -12 dB over the whole band.

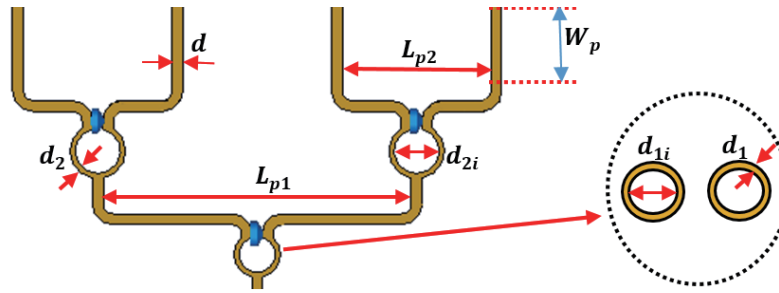


FIGURE 1. Geometry of the Wilkinson power divider.

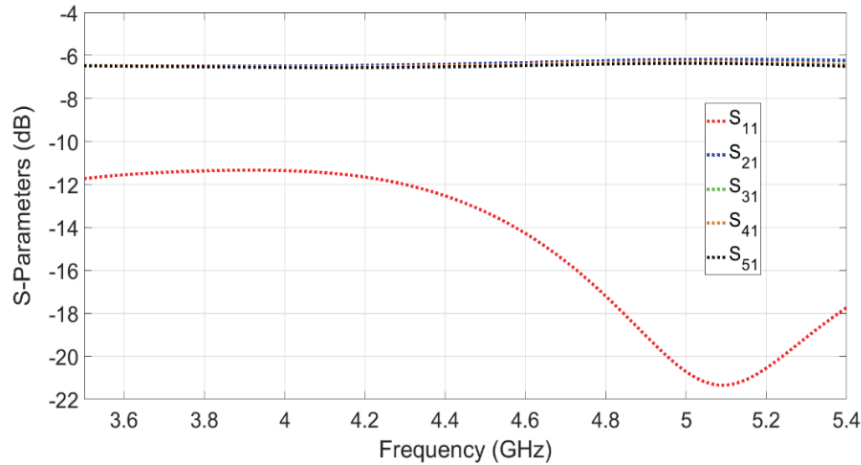


FIGURE 2. The simulated *S*-parameters of the Wilkinson power divider.

TABLE 1. Optimized dimensions for the proposed Wilkinson power divider (in mm).

Parameter	L_{p1}	L_{p2}	W_p	d	d_{1i}	d_1	d_{2i}	d_2
Value	64.9	31.3	18.5	2.3	3.836	1.9	9	1.5

TABLE 2. Optimized dimensions for the proposed single element (in millimeters).

Parameter	Value	Parameter	Value
W_1	16.8	R_1	14.5
W_2	15.18	R_2	13
W_3	15	R_3	11.65
W_4	15	R_4	10.43
W_5	15	R_5	9.34
W_6	15	R_6	8.35
R_7	7.47	a	60°

2.2. Single PLPDA Element

Figure 3 shows a schematic of a proposed single element. It is based on the LPDA scheme, where seven bow-tie dipoles are sequentially arranged in an alternative way on both the top and bottom substrate layers. The bow-tie element is selected for this design due to its superior bandwidth and ease of operating frequency tuning. The antenna is etched on a Roger RT5870 (Lossy) substrate with $\epsilon_r = 2.33$, $h = 0.787$ mm,

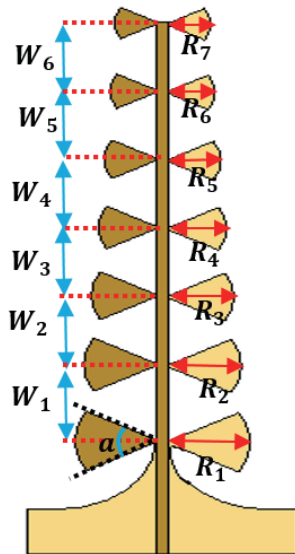
and $\tan \delta = 0.0012$. The overall optimized dimensions are tabulated in Table 2.

2.3. 4-Element PLPDA Bow-Tie-Based Array Structure

The first structure consists of a 4 element PLPDA bow-tie dipole based array as shown in Fig. 4. This design consists of a 4×1 linear array. Each radiating element consists of seven arms of bow-tie dipoles. The number of arms is cho-

TABLE 3. Optimized dimensions for the proposed antenna (in millimeters).

Parameter	L_{p1}	L_{p2}	d
Value	77.7	37.7	2.3

**FIGURE 3.** Geometry of the introduced single-element PLPDA bow-tie-based array structure.

sen as a compromise solution to maintain proper gain and keep the overall size within reasonable limits. The bow-tie arms are printed alternately on the top and bottom substrate layers. All dimensions are set according to Table 3. All dimensions are in mm. The overall dimensions of the proposed antenna are 160 mm \times 175 mm.

2.4. 4-Element PLPDA Bow-Tie-Based Array Structure with Triangle-Loading

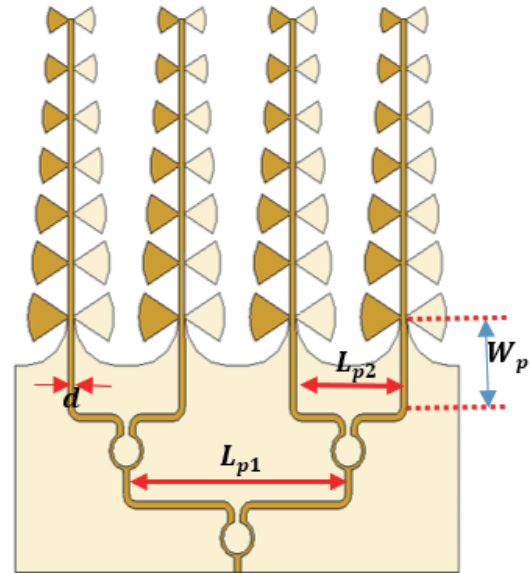
The second array adopts the same design as the first with triangle-shaped loading as shown in Fig. 5. The triangle-shaped resonators are placed in three successive rows in front of each antenna element. The second design is optimized to reduce the array size while maintaining a comparable gain to the first. The overall size is reduced to 134 mm \times 180 mm. The overall dimensions of the second design are tabulated in Table 4.

2.5. 4-Element PLPDA Bow-Tie-Based Array Structure with H-Loading

Figure 6 shows the third design, which is similar to the first design, but with two stacked rows of H-shaped resonators placed in front of the array radiating elements in both layers of the substrate. This structure is designed to achieve higher gain than the first structure, but the overall size of the array has been increased to be 160 mm \times 190 mm. The overall dimensions of the third design are tabulated in Table 5.

TABLE 4. Optimized dimensions for the proposed triangle shape (in millimeters).

Parameter	E_1	E_2	L_{p1}	L_{p2}	s
Value	16	8.77	64.9	31.3	6

**FIGURE 4.** Geometry of the introduced 4-element PLPDA bow-tie-based array structure.

3. RESULTS AND DISCUSSION

Prototypes of the proposed antenna arrays are fabricated on an RT/Duroid 5870 (lossy) substrate using thin film photolithography technique based on the design parameters given in the preceding section. A vector network analyzer (ROHDE & SCHWARZ ZVA 67) is used to measure the reflection coefficients and input impedances of the fabricated arrays. Fig. 7 shows photographs of the manufactured prototypes of the three proposed array designs (top and bottom views). A comparison of simulated and experimental reflection coefficients for the three design antennas is illustrated in Fig. 8. For the three cases, simulation and measurement results agree well.

The CSTMWS results for the first design, “the unloaded array”, presented in Fig. 8(a) reveals an impedance bandwidth (S_{11} less than -10 dB) extending from 3.5 GHz to 4.9 GHz, but for the HFSS, the bandwidth shrinks to be from 3.8 GHz to 5.1 GHz. The experimental result of this prototype realizes an impedance bandwidth of 1.4 GHz (3.7 GHz–5.1 GHz). The second design (triangular loaded), illustrated in Fig. 8(b), exhibits a CSTMWS bandwidth of 0.9 GHz (4.1 GHz–5 GHz), while the HFSS shows a little bit wider bandwidth of 1 GHz (4.3 GHz–5.3 GHz). An impedance bandwidth of 1 GHz (4.3 GHz–5.3 GHz) is achieved experimentally with this prototype. Finally, the third design case (H-shaped loaded), plotted in Fig. 8(c), has an impedance bandwidth of almost 1.2 GHz (3.8 GHz–5 GHz) according to both CSTMWS and HFSS simulators. The measured bandwidth shows very close

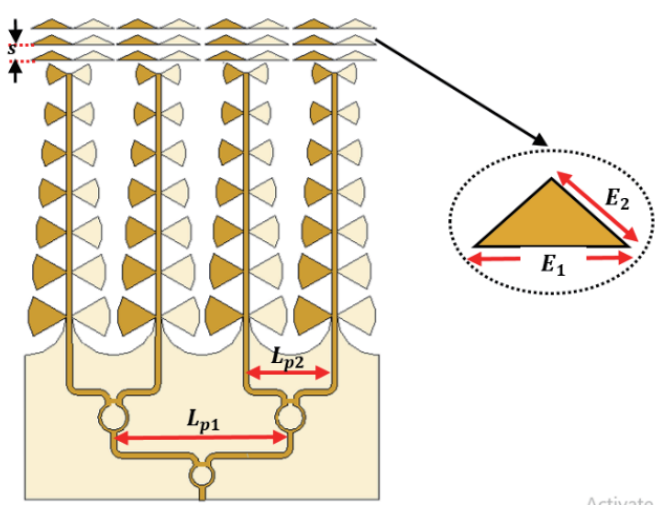


FIGURE 5. Geometry of the introduced 4-element PLPDA bow-tie-based array with triangle loading structure.

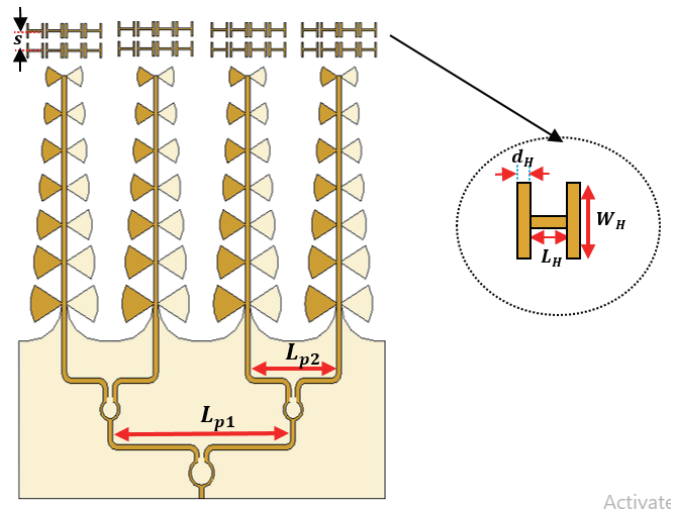


FIGURE 6. Geometry of the introduced 4-element LPDA bow-tie-based array with H-loading structure.

TABLE 5. Optimized dimensions for the proposed H shape (in millimeters).

Parameter	W_H	L_H	d_H	L_{p1}	L_{p2}	s
Value	6	6.19	0.81	81.7	39.7	7.19

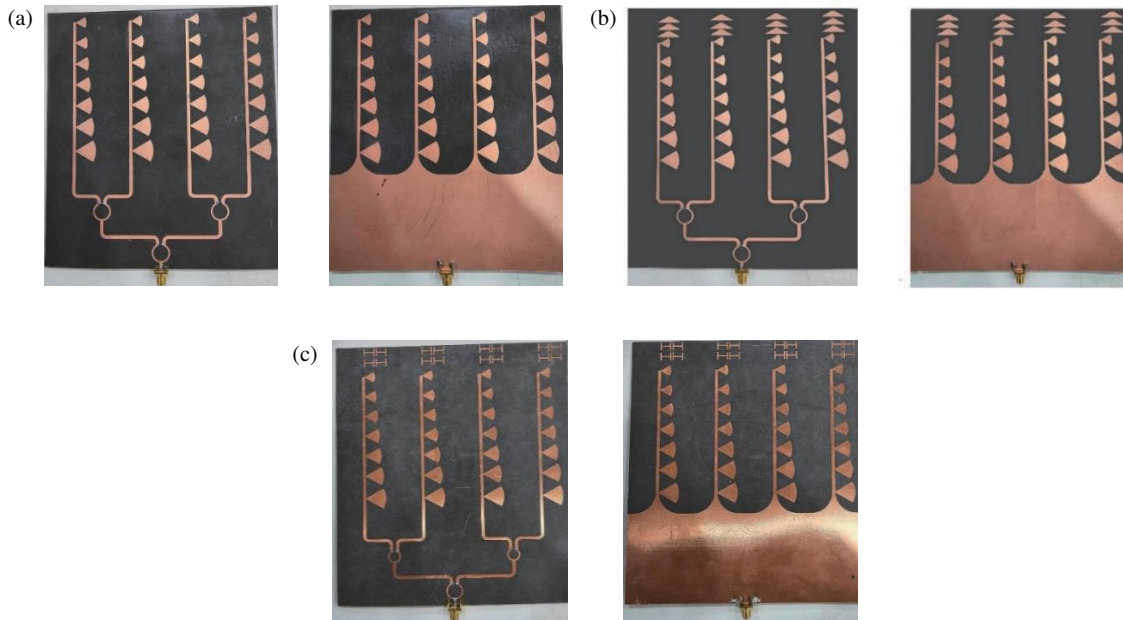


FIGURE 7. Photograph of the fabricated antennas (top and bottom view) (a) unloaded single PLPDA antenna element, (b) 4-element array of PLPDA with triangle-shape resonators, (c) 4-element array of PLPDA with H-shape resonators.

result to the simulation around 1.3 GHz, as it ranges from 3.7 GHz to 5 GHz.

In order to have deeper understanding of the radiation mechanism of the loaded arrays and how the loading affects the radiation performance, the current distributions of the unloaded single LPDA antenna element, the triangle loaded, and the H-shaped loaded arrays at 4.7 GHz are presented in Fig. 9. For

the single element, it can be noticed that the four middle three dipoles have the most contribution of the radiation. For the loaded cases presented in Figs. 8(b) and (c), the added resonators have some contribution to the overall array radiation.

These resonators can be considered as metamaterial with Epsilon Near Zero Index (ENZI) [1], where the phase velocity of propagating electromagnetic waves tends to infinity in ENZI

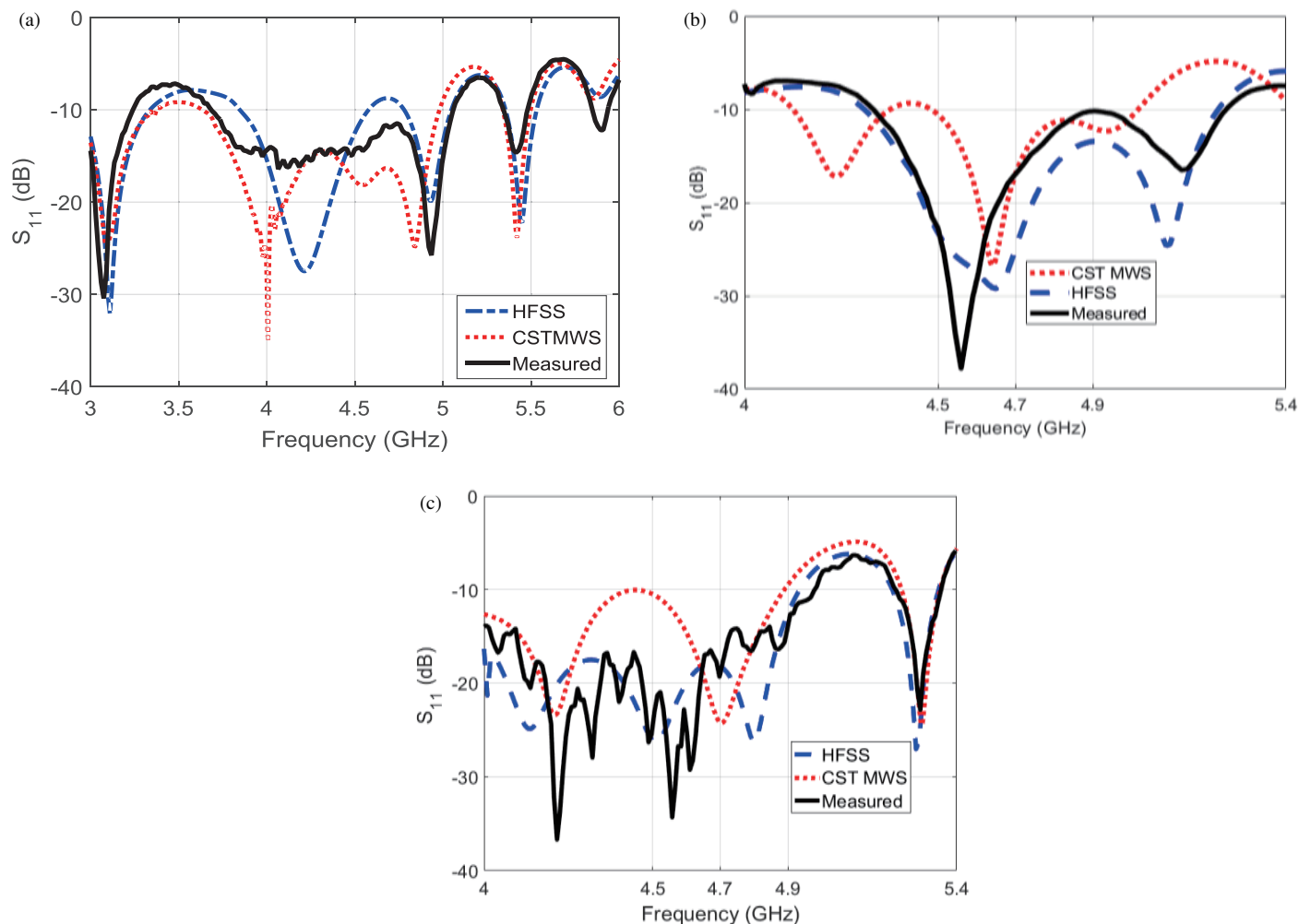


FIGURE 8. The simulated and measured reflection coefficients of (a) unloaded single PLPDA antenna element, (b) 4-element array of PLPDA with triangle-shape resonators, (c) 4-element array of PLPDA with H-shape resonators.

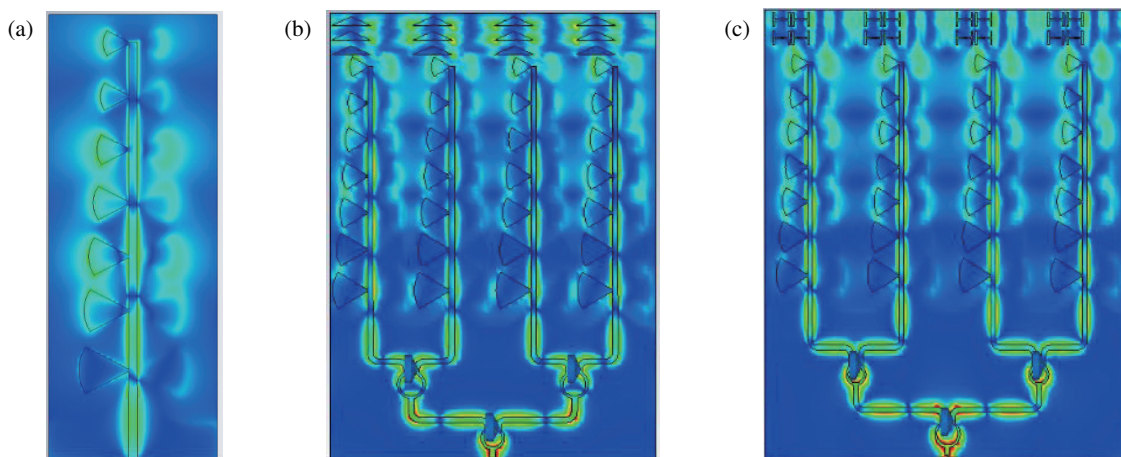
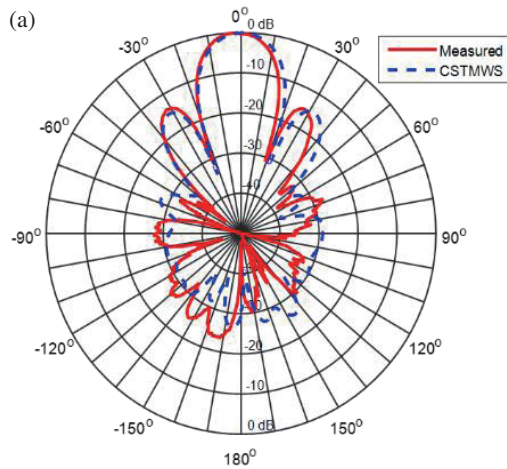


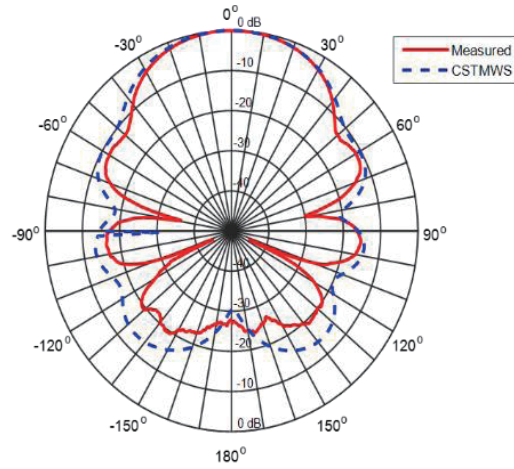
FIGURE 9. Current distributions of the proposed designs at 4.7 GHz for (a) unloaded single PLPDA antenna element, (b) 4-element array of PLPDA with triangle-shape resonators, (c) 4-element array of PLPDA with H-shape resonators.

metamaterials. In this situation, the wavelength of the electromagnetic field being manipulated by the ENZI metamaterial approaches infinity, resulting in the fields at the two ends of

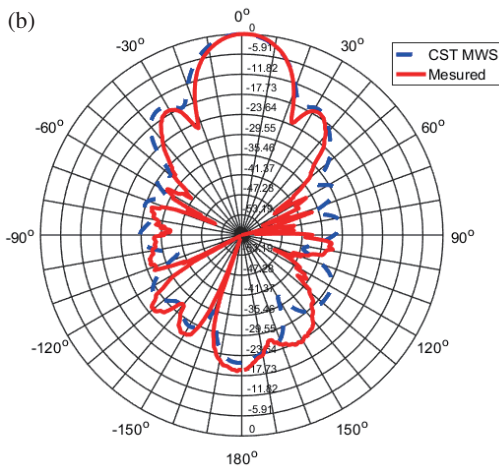
the slab becoming increasingly similar, which results in gain enhancement. Furthermore, they can also be considered as a lens focusing the radiating energy from the array and improv-



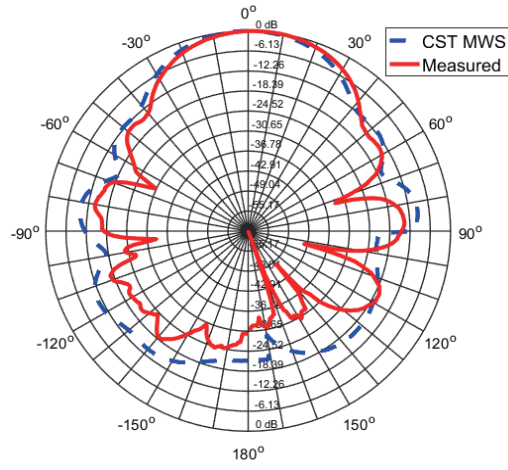
Azimuth Radiation Pattern at 4.7 GHz



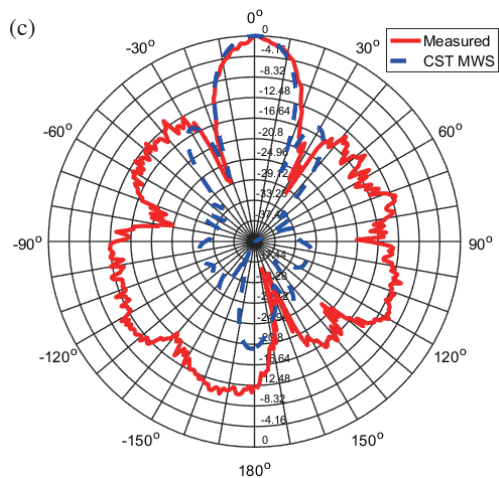
Elevation Radiation Pattern at 4.7 GHz



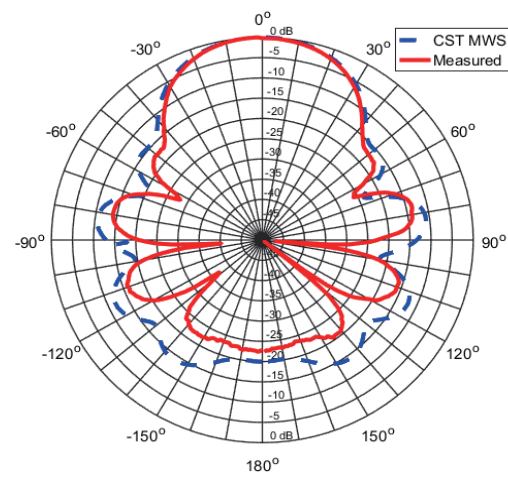
Azimuth Radiation Pattern at 4.7 GHz



Elevation Radiation pattern at 4.7 GHz



Azimuth Radiation Pattern at 4.7 GHz



Elevation Radiation Pattern at 4.7 GHz

FIGURE 10. The simulated and measured radiation pattern for for (a) 4-element PLPDA bow-tie array, (b) 4-element array of PLPDA with triangle-shape resonators, (c) 4-element array of PLPDA with H-shape resonators.

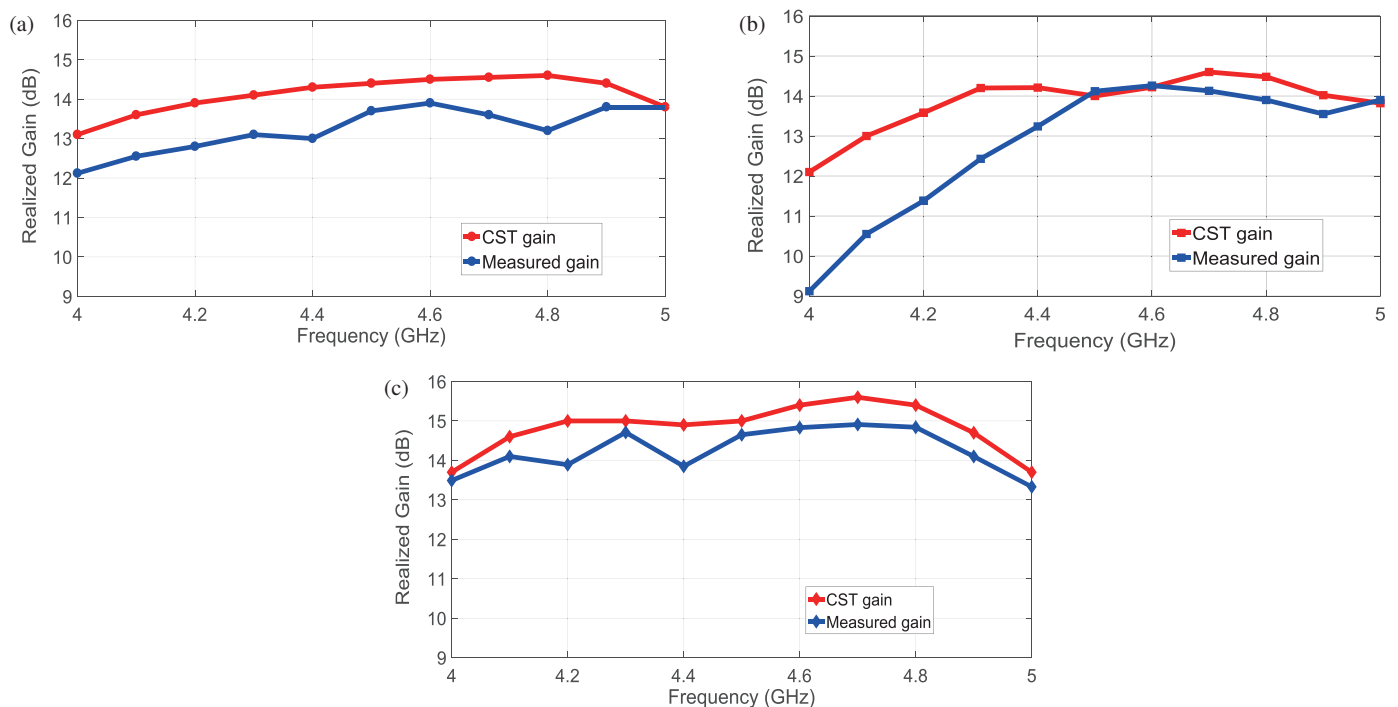


FIGURE 11. The measured gain vs. CSTMWS simulation gain for (a) 4-element PLPDA bow-tie array, (b) 4-element array of PLPDA with triangle-shape resonators, (c) 4-element array of PLPDA with H-shape resonators.

ing the aperture efficiency of the array system. Moreover, it can be noticed that at lower frequency of the band (i.e., 4 GHz) the bigger sized dipoles have more contribution in the overall radiation. However, at higher frequency of the band (i.e., 5 GHz) the smaller dipoles will have much more contribution. Both simulated and measured radiation patterns, E-plane and H-plane, of the proposed arrays at 4.7 GHz are presented in Fig. 10. CSTMWS and measured radiation patterns agree very well for all designs at 4.7 GHz. However, some discrepancies can be figured out in the sidelobes which can be accounted for some undesired reflection inside the anechoic chamber and some minor fabrication imperfections in the arrays.

It can be noticed that the unloaded LPDA array has beamwidths of 21 degrees, and 45 degrees in *E*- and *H*-planes, respectively, while the beamwidths for the triangle loaded PLPDA are 45 and 20 degrees. For H-loaded PLPDA, it has beamwidths of 18 and 45 degrees. The three proposed designs achieve sidelobe levels (SLLs) of -14 dB, -17 dB, and -13 dB, respectively. In terms of the total realized gain (measured), the three prototypes exhibit maximum gain of 13.8 dBi for the unloaded PLPDA, 14.1 dBi and 15 dBi for the loaded arrays at 4.7 GHz.

The three arrays exhibit a broad-side directive patterns in both the *E*-plane and *H*-plane with good stability of the radiation pattern over the operating bandwidth.

The total realized gain comparison between the measured and CSTMWS is plotted in Fig. 11 for the three cases. It can be concluded that the gain at 4.7 GHz is enhanced by about 0.5 dB for the triangle loaded case and by almost 1 dB in the case of the introduction of the H-shaped resonators compared to the unloaded array.

4. CONCLUSION

Three different C-band (4 GHz–5 GHz) directive antenna arrays are presented. Array loading principle using triangle-shaped and H-shaped resonators is investigated. Gain enhancement of 0.5 dB and 1 dB at 4.7 GHz is achieved for the loaded arrays. Very good agreement is achieved between simulated and experimental results for impedance bandwidth and radiation patterns. A total realized gain of almost 15 dBi at 4.7 GHz is achieved in the H-shaped loaded array. Three array prototypes can be considered as very good candidates for various high-fidelity C-band communication applications requiring high signal-to-noise ratio.

REFERENCES

- [1] Shehata, R. E. A., M. Hindy, H. Elmekati, and A. M. F. Elboushi, "Design of a beam-steering metamaterial inspired LPDA array for 5G applications," *Progress In Electromagnetics Research M*, Vol. 117, 151–161, 2023.
- [2] Abd El-Hameed, A. S., E. G. Ouf, A. Elboushi, A. G. Seliem, and Y. Izumi, "An improved performance radar sensor for K-band automotive radars," *Sensors*, Vol. 23, No. 16, 7070, Aug. 2023.
- [3] Shehata, G. S., A. S. A. El-Hameed, S. M. Ebrahim, M. A. Mohana, and A. M. Abbas, "Bow-tie antenna with improved performance for advanced GPR applications," *International Journal of Microwave & Optical Technology*, Vol. 18, No. 3, 266–274, May 2023.
- [4] El-Nady, S., R. R. Elsharkawy, A. I. Afifi, and A. S. A. El-Hameed, "Performance improvement of substrate integrated cavity fed dipole array antenna using ENZ metamaterial for 5G applications," *Sensors*, Vol. 22, No. 1, 125, 2022.

- [5] El-Hameed, A. S. A. and M. Sato, "Antenna array for Ku-band MIMO GB-SAR," *IEEE Access*, Vol. 9, 29 565–29 572, Feb. 2021.
- [6] Isbell, D., "Log periodic dipole arrays," *IRE Transactions on Antennas and Propagation*, Vol. 8, No. 3, 260–267, May 1960.
- [7] Wang, B., A. Chen, and D. Su, "An improved fractal tree log-periodic dipole antenna," in *2008 Asia-Pacific Symposium on Electromagnetic Compatibility and 19th International Zurich Symposium on Electromagnetic Compatibility*, 831–834, Singapore, May 2008.
- [8] Dhruva, T. V., J. A. Baskaradas, and K. G. S. Narayan, "Analysis of half-wave dipole antenna with various bending angles," in *2021 IEEE Indian Conference on Antennas and Propagation (InCAP)*, 454–457, Dec. 2021.
- [9] Erman, F., E. Hanafi, E.-H. Lim, W. A. W. M. Mahyiddin, S. W. Harun, H. Umair, R. Soboh, and M. Z. H. Makmud, "Miniature compact folded dipole for metal mountable UHF RFID tag antenna," *Electronics*, Vol. 8, No. 6, 713, Jun. 2019.
- [10] Purwono, A., V. Dear, K. Huda, and I. Setyawan, "Configuration of inverted-V dipole NVIS HF antenna for offshore fast patrol boat," in *2022 11th Electrical Power, Electronics, Communications, Controls and Informatics Seminar (EECCIS)*, 181–184, Aug. 2022.
- [11] Ebihara, S., H. Hanaoka, T. Okumura, and Y. Wada, "Interference criterion for coaxial-fed circular dipole array antenna in a borehole," *IEEE Transactions on Geoscience and Remote Sensing*, Vol. 50, No. 9, 3510–3526, Sep. 2012.
- [12] Tziris, E. N., P. I. Lazaridis, Z. D. Zaharis, J. P. Cosmas, K. K. Mistry, and I. A. Glover, "Optimized planar elliptical dipole antenna for UWB EMC applications," *IEEE Transactions on Electromagnetic Compatibility*, Vol. 61, No. 4, 1377–1384, Aug. 2019.
- [13] Faouri, Y. S., S. Ahmad, N. O. Parchin, C. H. See, and R. Abd-Alhameed, "A novel meander bowtie-shaped antenna with multi-resonant and rejection bands for modern 5G communications," *Electronics*, Vol. 11, No. 5, 821, Mar. 2022.
- [14] Tawk, Y., K. Y. Kabalan, A. El-Hajj, C. G. Christodoulou, and J. Costantine, "A simple multiband printed bowtie antenna," *IEEE Antennas and Wireless Propagation Letters*, Vol. 7, 557–560, Jun. 2008.
- [15] Wang, B., A. Chen, and D. Su, "An improved fractal tree log-periodic dipole antenna," in *2008 Asia-Pacific Symposium on Electromagnetic Compatibility and 19th International Zurich Symposium on Electromagnetic Compatibility*, 831–834, Singapore, May 2008.
- [16] Anagnostou, D. E., J. Papapolymerou, M. M. Tentzeris, and C. G. Christodoulou, "A printed log-periodic Koch-dipole array (LPKDA)," *IEEE Antennas and Wireless Propagation Letters*, Vol. 7, 456–460, Jun. 2008.
- [17] Chen, J., J. Ludwig, and S. Lim, "Design of a compact log-periodic dipole array using T-shaped top loadings," *IEEE Antennas and Wireless Propagation Letters*, Vol. 16, 1585–1588, Jan. 2017.
- [18] Chang, L., S. He, J. Q. Zhang, and D. Li, "A compact dielectric-loaded log-periodic dipole array (LPDA) antenna," *IEEE Antennas and Wireless Propagation Letters*, Vol. 16, 2759–2762, Aug. 2017.
- [19] Hsu, H.-T. and T.-J. Huang, "A koch-shaped log-periodic dipole array (LPDA) antenna for universal ultra-high-frequency (UHF) radio frequency identification (RFID) handheld reader," *IEEE Transactions on Antennas and Propagation*, Vol. 61, No. 9, 4852–4856, Sep. 2013.
- [20] Haraz, O. M., S. A. Alshebeili, and A.-R. Sebak, "Low-cost high gain printed log-periodic dipole array antenna with dielectric lenses for V-band applications," *IET Microwaves, Antennas & Propagation*, Vol. 9, No. 6, 541–552, Apr. 2015.
- [21] Marathe, D. and K. Kulat, "A compact triple-band negative permittivity metamaterial for C, X-band applications," *International Journal of Antennas and Propagation*, Vol. 2017, Article ID 7515264, Oct. 2017.
- [22] Kubacki, R., S. Lamari, M. Czyzewski, and D. Laskowski, "A broadband left-handed metamaterial microstrip antenna with double-fractal layers," *International Journal of Antennas and Propagation*, Vol. 2017, Article ID 6145865, May 2017.
- [23] Sievenpiper, D., L. Zhang, R. F. J. Broas, N. G. Alexopoulos, and E. Yablonovitch, "High-impedance electromagnetic surfaces with a forbidden frequency band," *IEEE Transactions on Microwave Theory and Techniques*, Vol. 47, No. 11, 2059–2074, Nov. 1999.
- [24] Rahmadani, F. and A. Munir, "Microstrip patch antenna miniaturization using artificial magnetic conductor," in *2011 6th International Conference on Telecommunication Systems, Services, and Applications (TSSA)*, 219–223, Oct. 2011.
- [25] Foroozesh, A. and L. Shafai, "Investigation into the application of artificial magnetic conductors to bandwidth broadening, gain enhancement and beam shaping of low profile and conventional monopole antennas," *IEEE Transactions on Antennas and Propagation*, Vol. 59, No. 1, 4–20, Jan. 2011.
- [26] Cook, B. S. and A. Shamim, "Utilizing wideband AMC structures for high-gain inkjet-printed antennas on lossy paper substrate," *IEEE Antennas and Wireless Propagation Letters*, Vol. 12, 76–79, Jan. 2013.
- [27] Kwon, O. H., S. Lee, J. M. Lee, and K. C. Hwang, "A compact, low-profile log-periodic meandered dipole array antenna with an artificial magnetic conductor," *International Journal of Antennas and Propagation*, Vol. 2018, 1–10, Jun. 2018.
- [28] Syed, A., M. Sheikh, M. T. Islam, and H. Rmili, "Metamaterial-loaded 16-printed log periodic antenna array for microwave imaging of breast tumor detection," *International Journal of Antennas and Propagation*, Vol. 2022, 1–15, Sep. 2022.